

Construction of Two-Dimensional Chiral Networks through Atomic Bromine on Surfaces

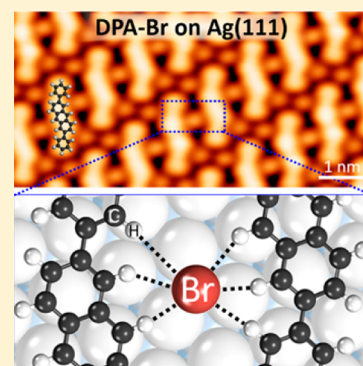
Jianchen Lu,^{†,§} De-Liang Bao,^{†,§} Huanli Dong,^{‡,§} Kai Qian,[†] Shuai Zhang,[†] Jie Liu,[‡] Yanfang Zhang,[†] Xiao Lin,^{*,†} Shi-Xuan Du,^{*,†} Wenping Hu,[‡] and Hong-Jun Gao[†]

[†]Institute of Physics & University of Chinese Academy of Sciences, Chinese Academy of Sciences, Beijing 100190, P. R. China

[‡]Institute of Chemistry, Chinese Academy of Sciences, Beijing 100190, P. R. China

Supporting Information

ABSTRACT: Using atomic bromine and 2,6-diphenylanthracene (DPA), we successfully constructed and characterized the large-area 2D chiral networks on Ag(111) and Cu(111) surfaces by combining molecular beam epitaxy with scanning tunneling microscopy. The Br atoms distribute themselves periodically in the network with the maximum number of $-C-H\cdots Br$ hydrogen bonds. Density functional theory calculations demonstrate that the hydrogen bonds contribute to the stability of the Br-organic networks. In addition, by controlling the ratio of bromine atoms to DPA molecules, different patterns of Br-organic networks were obtained on Ag(111) surfaces. Further experiments with 2,6-di(4-cyclohexylphenyl)anthracene on Ag(111) produced analogous atomic bromine guided 2D chiral networks.



Investigation of supramolecular architectures can pave the way for rational design of building blocks that can mimic natural assemblies.¹ Two-dimensional supramolecular architectures constitute a significant category due to their dramatic new characteristic applications in the fields of nanoscience and nanotechnology.^{2–7} Benefiting from high purity and controllable interactions, most 2D supramolecular architectures are typically obtained by “bottom up” nanofabrication based on molecular self-assembly.^{7,8} In general, self-assembled monolayers (SAMs) of organic molecules are classified into single-component systems^{9,10} and multicomponent systems.^{11,12} The latter are more interesting due to the more complex combinations resulting in the widely varied structures and novel properties.¹² Among the multicomponent systems, multimolecule constructed SAM networks are surpassed by adatom-mediated SAM networks, which have the advantages of more diverse interactions and more convenient manipulation of configuration due to their simplicity, flexibility, and the wide availability of their components.^{13–15} Most reported work on adatom-mediated SAMs focuses on single metal atoms, including transition-metal atoms, for instance, Fe,^{13,16} Cu,^{17,18} Mn,¹⁹ Co,²⁰ and Ni,²¹ and alkali metal atoms, for instance, K²² and Cs.²³ Although the addition of metal atoms coordinates the SAM systems effectively, the strong metallicity of metal atoms induces electronic states near the Fermi level of the whole system.^{19,24,25} This changes the semiconducting properties of organic 2D supramolecular architectures and limits their applications.

In contrast, nonmetal atoms produce less effect on the whole 2D SAM system because of weak electrostatic interaction. However, to date, such self-assembled networks are rarely

reported. Sun et al. reported that quaterphenyl molecules could be arranged by oxygen atoms into a nanostructure, but the size of such a structure is limited.²⁶ Therefore, to achieve the intrinsic properties, it is important to grow large-scale, high-quality, highly ordered 2D self-assembled networks mediated by nonmetal atoms.

Here we report atomic bromine-mediated self-assembled 2D chiral networks of 2,6-diphenylanthracene (DPA) molecules on a Ag(111) surface. Four kinds of large-scale and highly ordered self-assembled Br-organic networks were obtained. We find that the stability of the self-assembled structures benefits from the maximum number of hydrogen bonds between the DPA molecules and bromine atoms. Density functional theory (DFT) calculations demonstrate that the hydrogen bonds, $-C-H\cdots Br$, contribute to the formation of the Br-organic networks. Atomic bromine-mediated self-assembled 2D networks were achieved in other systems, for example, DPA/Cu(111) and 2,6-di(4-cyclohexylphenyl)anthracene (DcC₆PA)/Ag(111).

After deposition of the bromine atoms and DPA molecules on the Ag(111) surface (see Supporting Information for detailed method), we observed a large-scale, highly ordered self-assembled structure (Structure I), as shown in Figure 1A. (The chemical structure of DPA molecule is illustrated in the bottom right of Figure 1A, composed of 26 carbon atoms and 18 hydrogen atoms.) Scanning tunneling microscopy (STM)

Received: November 16, 2016

Accepted: December 23, 2016

Published: December 23, 2016

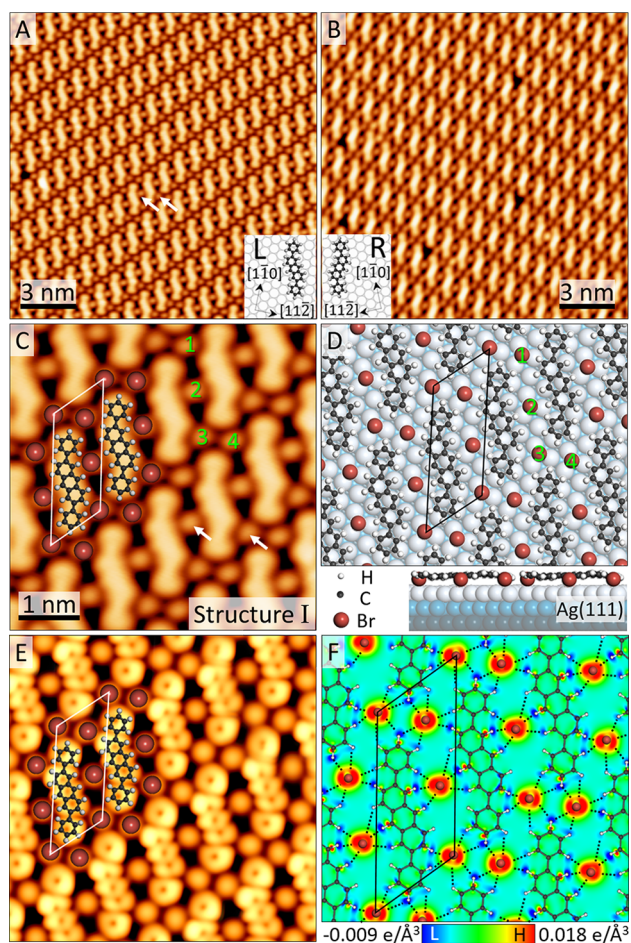


Figure 1. Structure I of atomic bromine-mediated self-assembled DPA molecular network on Ag(111) surface. (A,B) Large-area L-chiral (A) and R-chiral (B) domains of the networks. The insets of (A) and (B) are the chemical structures of L-chiral and R-chiral DPA molecules, respectively. (C) High-resolution STM image of the L-chiral network, superimposed by a proposed model. The brown spots are bromine atoms. (D,E) DFT-optimized adsorption configurations of structure I (D) and corresponding simulated STM image (E). (F) Theoretical calculated charge density difference of the Br-DPA hydrogen bond networks. Red and blue parts indicate the distribution of positive charge and negative charge, respectively. The black dashed lines represent the possible $-C-H\cdots Br$ hydrogen bonds between DPA molecules and Br atoms. Scanning parameters: (A) $V_s = -0.5$ V, $I_t = 0.8$ nA; (B) $V_s = -2.0$ V, $I_t = 0.2$ nA; (C) $V_s = -0.5$ V, $I_t = 2$ nA.

appearance of the DPA monomer is clearly resolved in the high-resolution STM image of Figure 1C (a zoom-in STM image of Figure 1A). Besides the DPA molecules, there exist many regularly arranged bright dots (marked by white arrows) between DPA molecules in Figure 1A,C. We assign these dots as represent Br atoms originating from the dissociation of HBr gas. In Figure 1C, models of two DPA molecules and several bromine atoms (the brown balls) are superimposed to show the periodicity of the self-assembled superstructure, and a unit cell (including one DPA molecule and three bromine atoms) is indicated by the white parallelogram. The three bromine atoms (labeled 1, 2, and 3 in Figure 1C) have an equally spaced arrangement with a distance of 7.7 Å, which is very close to the $\sqrt{7}$ times Ag(111) lattice parameter (a_{Ag}), that is, $\sqrt{7} \times a_{Ag}$ (2.90 Å) = 7.67 Å. The two bromine atoms (labeled 3 and 4) are separated by 5.1 Å, which is approximately $\sqrt{3}$ times a_{Ag}

that is, $\sqrt{3} \times a_{Ag}$ (2.90 Å) = 5.02 Å. Furthermore, we also have imaged the substrates exposed only to the bromine atoms. The bromine atoms themselves form chains on the Ag(111) surfaces, as shown in Figure S1. It is different from the previous report about Br deposited on Ni(110), where the bromine atoms will form ordered rows with Ni atoms.²⁷

To gain further insight into this highly ordered self-assembled structure, we carried out DFT calculations. Figure 1D shows the optimized adsorption geometry of DPA molecules and bromine atoms on Ag(111) surface. In the top view, all bromine atoms sit on the hollow sites of Ag(111) surfaces, and three equally spaced Br atoms labeled 1, 2 and 3 (two Br atoms, labeled 3 and 4), follow the $\sqrt{7}$ direction ($\sqrt{3}$ direction) of Ag(111) substrate, which fits well with the STM results (Figure 1C). (For the height difference analysis, see Figure S2.) On the basis of Figure 1D, we obtained a simulated STM image (Figure 1E), which agrees very well with the experimental STM image (Figure 1C). It is noteworthy that in our results all Br atoms are located on the hollow sites of the substrate, which are the most stable adsorption sites for single bromine atom on Ag(111). This is different from previous report that bromine atoms adsorbed at the bridge sites of Au(111) due to strong interaction with Au adatoms.²⁸

To further explore the origin of the interaction between Br atoms and organic molecules, the charge density difference of the self-assembled structure was calculated, as shown in Figure 1F, where the DPA molecule models and Br atoms (brown balls) are overlaid to indicate the positions of atoms. It clearly shows that the regions of high-electronegativity Br atoms are electron-rich sites (red parts) and the region of low-electronegativity H atoms are electron-deficient sites (blue parts). An attractive electrostatic interaction between negatively charged Br atoms and positively charged H atoms is expected. On the basis of the charge density difference data, we sketched out the possible electrostatic interactions ($-C-H\cdots Br$) by the black dashed lines in the Figure 1F. It is plain to see that the highly ordered self-assembled network is stabilized by the $-C-H\cdots Br$ unconventional hydrogen bonds; that is, large-scale 2D Br-organic hydrogen bond networks have been successfully constructed. In addition, six hydrogen bonds per Br atom can be counted in the Figure 1F. More importantly, six hydrogen bonds is the maximum in the structure, as can be seen by considering the possible adsorption sites of Br atoms and DPA molecules on Ag(111) surface. We propose that the nonmetal atomic Br-mediated 2D self-assembled network is dominated by forming more hydrogen bonds between Br atoms and H atoms, that is, the maximum number of hydrogen bonds.

Moreover, because of the prochirality of DPA on the surfaces, the DPA molecule should exhibit two enantiomers (L-DPA and R-DPA) on the Ag(111) substrate. In Figure 1A, all DPA molecules have the same chirality (L-DPA, labeled by L in the bottom-right of Figure 1A), which reveals chiral selectivity²⁹ during the formation of 2D self-assembled networks. We denote it as L-domain. The large-scale R-domain composed of R-DPA molecules (R-DPA, labeled by R in the bottom left of Figure 1B) and bromine atoms is shown in the Figure 1B, which has the same size unit cell as the L-domain. In addition, the self-assembled structures of the pristine DPA on Ag(111) have been presented in the Figure S5.

On the same surface, adjusting the ratio of bromine atoms to DPA molecules by increasing (or decreasing) the pressure (or exposure time) of HBr gas, we obtained different 2D Br-DPA self-assembled networks. Figure 2A is a large-scale STM image

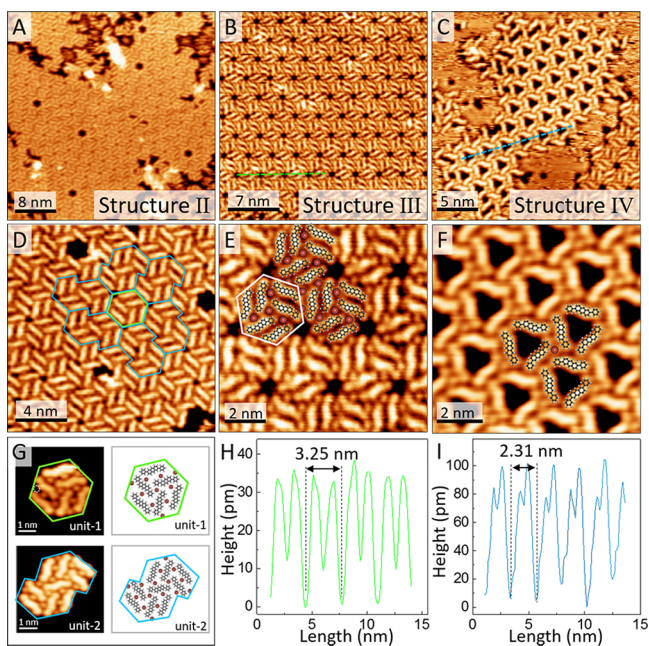


Figure 2. Structures II, III, and IV of Br-DPA networks on Ag(111) surfaces. (A–C) Large-scale STM images showing three different structures (A, structure II; B, structure III; C, structure IV). (D) Close-up STM image of the structure II showing that the structure is composed of two kinds of units, unit-1 and unit-2. The light-green (light-blue) contour indicates unit-1 (unit-2). (E,F) Zoom-in STM images of structures III (E) and IV (F). (G) The upper and lower panels show the high-resolution STM image (left) and the related schematic structure (right) of unit-1 and unit-2, respectively. (H,I) The line profiles along the green dashed line in (B) and the blue dashed line in (C) showing the periodicities of the hole in structures III (H) and IV (I), respectively. Scanning parameters: (A) $V_s = -3$ V, $I_t = 0.05$ nA; (B) $V_s = -2$ V, $I_t = 0.03$ nA; (C) $V_s = -3$ V, $I_t = 0.10$ nA; (D) $V_s = -1$ V, $I_t = 0.05$ nA; (E) $V_s = -2$ V, $I_t = 0.03$ nA; and (F) $V_s = -3$ V, $I_t = 0.10$ nA.

showing the locally well-defined network structure (structure II), which is composed of two kinds of units, unit-1 and unit-2. For closer inspection of the structure II, a magnified view is displayed in Figure 2D, where the light-green and the light-blue contours show shapes of unit-1 and unit-2, respectively. Moreover, the Br atoms are the connectors between different units. The left parts of Figure 2G show the high-resolution STM images of unit-1 and unit-2. From the schematic structures (right parts of Figure 2G), we find that the Br atoms only reside in certain positions relative to the DPA molecules, that is, the sites of junctions of three DPA molecules and kink sites of DPA molecules, where Br atoms can form more hydrogen bonds with H atoms of the molecules, that is, the maximum number of hydrogen bonds. In addition, Figure 2B,E shows another atomic Br-mediated 2D self-assembled network (structure III), which has periodic holes in the triangular lattice. The periodicity is determined from the line profile to be 3.25 ± 0.05 nm (Figure 2H). Some DPA molecule models and Br atoms are overlaid onto Figure 2E to guide the eye. This clearly shows a highly ordered structure, where the unit is marked by the white hexagon. In the unit, six identical chiral DPA molecules are connected by four Br atoms and the Br atoms occupy only the positions of three molecular junctions, which meets the requirement of maximizing the number of hydrogen bonds. Another structure (structure IV) is also observed, as shown in Figure 2C,F, which exhibits a periodic hole structure with the periodicity of 2.31 ± 0.05 nm,

as indicated in the line profile of Figure 2I. Obviously, the Br atoms reside in the positions where the maximum number of hydrogen bonds can be formed. In addition, the schematic structural models for structures II, III, and IV are shown in Figure S3, where the bromine atoms all locate on fcc/hcp sites of Ag(111) substrate, the same as with structure I. Until now, we have fabricated four types of 2D Br-DPA networks on the Ag(111) surface. The ratio of Br atoms to DPA molecules for structures I, II, III, and IV is 3:1, 5:3, 4:3, and 1:3, respectively, as shown in Table S1. (For the control of selective formation of four networks, see the Supporting Information.)

To check the range of possibilities of atomic bromine mediated self-assembled networks, we repeated the experiment with the same DPA molecules but on a different surface, Cu(111). Similar to the procedures with the Ag(111) substrate, the bromine atoms and DPA molecules were deposited onto Cu(111) surfaces. As shown in Figure 3A, a well-defined self-

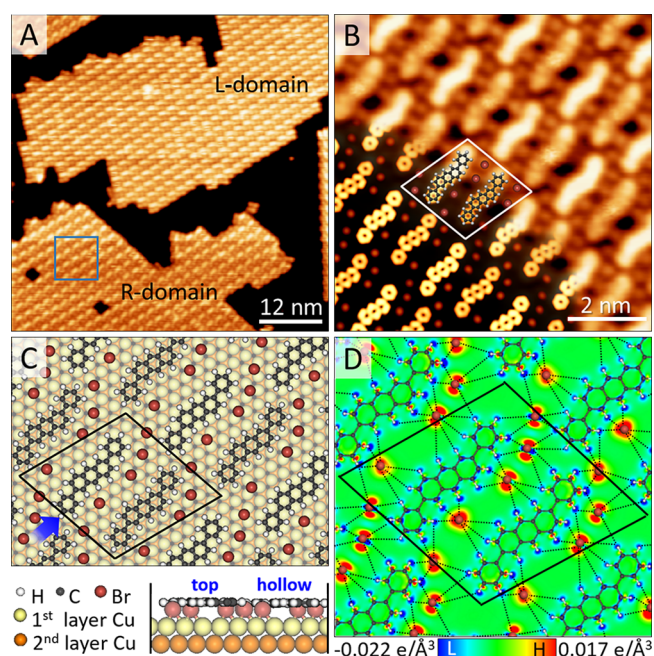


Figure 3. Br-DPA network on Cu(111). (A) Large-area STM image of atomic bromine-mediated self-assembled hydrogen-bond network on Cu(111) surface. The upper (lower) island is an L-chiral DPA (R-chiral DPA) domain. (B) (Upper-right) Close-up STM image of (A) with a unit cell marked by a white parallelogram. (Lower-left) Theoretically simulated STM image. (C) Top view and side view (along the direction of blue arrow) of DFT-optimized adsorption configurations of Br-DPA hydrogen-bond network on Cu(111). There are two kinds of DPA molecules, named “top” and “hollow”. (D) Theoretically calculated charge density difference of the Br-DPA hydrogen bond network on Cu(111). The black dashed lines indicate the possible $-C-H \cdots Br$ hydrogen bonds. Scanning parameters: (A) $V_s = -1.0$ V, $I_t = 0.05$ nA; (B) $V_s = -1.0$ V, $I_t = 0.5$ nA.

assembled structure was obtained. For deeper inspection, a close-up view of the blue-framed region in Figure 3A is displayed in the upper-right part of Figure 3B, where the DPA molecules are clearly observed. However, the heights (brightness) of the molecules are not identical but are arranged with alternating bright and dark molecules. Bromine atoms sit between molecules, similar to the Ag(111) case. The white rhombus in Figure 3B represents the unit cell, where left (right) is the bright (dark) DPA molecule. The above discussion

focuses on the R-DPA domain (lower part of Figure 3A,B). Note that the upper part of Figure 3A is L-DPA domain. The atomic resolution STM images about the R-DPA domain, the L-DPA domain, and the domain boundary are shown in Figure S4.

To investigate the configuration of Br-DPA network on the Cu(111) surface in detail, we carried out calculations based on DFT. The upper panel of Figure 3C shows the optimized adsorption configuration with a unit cell marked by the black rhombus. Obviously, two molecular adsorption configurations coexist in one unit cell. In one, the centers of benzene rings are on the top sites of the underlying Cu atoms, named “top-molecule”, and in the other, the centers of benzene rings are on the hollow sites of the underlying Cu atoms, named “hollow-molecule”. The side view of optimized structures in the direction of blue arrow (the lower panel in Figure 3C) presents the apparent height difference of two types of DPA molecules with 3.0 Å for top-molecule and 2.9 Å for hollow-molecule, which is the reason for the observed alternating bright and dark molecules in Figure 3B. On the basis of the optimized configuration, we obtained a simulated STM image (lower-left part of Figure 3B) and merged it with an experimental STM image (upper-right part of Figure 3B). The simulated image shows excellent agreement with the experimental results. Figure 3D shows the calculated charge density difference. Just as in the same analysis of a sample on Ag(111) surfaces, the self-assembled structure of DPA molecules and bromine atoms on the Cu(111) surfaces is dominated by hydrogen bonds between Br atoms and H atoms. The bromine atoms, here again, sit on the junctions of three DPA molecules and at the kink sites of DPA molecules, where the number of hydrogen bonds can reach the maximum. In brief, the atomic bromine-mediated chiral self-assembled network structures on the Cu(111) substrate were constructed, and the positions of Br atoms meet the requirement of maximizing the number of hydrogen bonds.

Also, another kind of molecule, (DcC₆PA), was used to form atomic bromine-mediated 2D chiral hydrogen bonds network structure on Ag(111) surfaces. Compared with DPA, DcC₆PA molecule has two extra cyclohexanyl groups at each end of the DPA molecule, as illustrated in Figure 4A. By deposition of Br atoms and DcC₆PA molecules onto the Ag(111) surface, we obtained a well-defined structure (Figure 4B, with a unit cell marked by a black parallelogram), where the DcC₆PA monomer is clearly identified: two bright protrusions representing two cyclohexanyls. Meanwhile, the bromine atoms exist among DcC₆PA molecules with an alternating number arrangement with 3,1,3,1..., as indicated by the green arrow and three blue arrows. The alternate pattern is more easily identified in the close-up image (Figure 4C), in which a schematic of molecular structure and Br atoms is overlaid to highlight the atomic positions. (See Figure S6 for self-assembled structures of pristine DcC₆PA on Ag(111).) Just as in Br-DPA on Ag(111) and Cu(111) surfaces, the Br atoms in the Br-DcC₆PA on Ag(111) surfaces are on the junctions of three DcC₆PA molecules and at the kink sites of DcC₆PA molecules. The green dashed lines (Figure 4C) indicate the possible hydrogen bonds between Br atoms and H atoms. Therefore, we confirmed that the atomic bromine-mediated self-assembled network can also be achieved with DcC₆PA molecules, and the Br atoms sit on the special sites where the maximum number of hydrogen bonds can be formed. Figure 4D shows a schematic structural model of the 2D hydrogen-

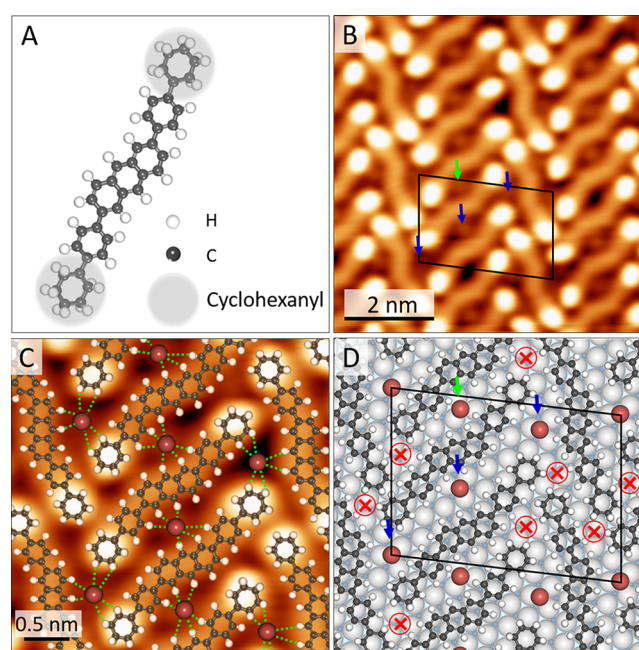


Figure 4. Br-DcC₆PA network on Ag(111). (A) Chemical structure of DcC₆PA molecule. (B) STM image of Br-DcC₆PA network on Ag(111) surface. One green and three blue arrows indicate the positions of Br atoms. (C) Zoom-in STM image superimposed by a schematic models. The green dashed lines denote the possible hydrogen bonds. (D) Schematic structural models. The red circles with a cross inside indicate positions where the Br atoms cannot reside because of the space limitation. Scanning parameters: (B) $V_s = -1.0$ V, $I_t = 0.05$ nA; (C) $V_s = -1.0$ V, $I_t = 0.5$ nA.

bond network structure of Br-DcC₆PA on Ag(111) surface. The positions of red circles with a cross inside are also junction sites; however, no bromine atoms are observed there. This absence of bromine atoms may be attributable to the fact that there is not enough room.

It should be mentioned that the 2D chiral halogen-coordination networks formed here are different from the previous reports about the self-assembled patterns of bromine substituted polyaromatic hydrocarbon. Actually, 2D self-assembly of polyaromatic hydrocarbon guided and stabilized by halogen bonds, especially for intermolecular Br...Br halogen bonds and $-C-H\cdots Br-C-$ hydrogen bonds, has been widely studied in recent years.^{28,30–37} For instance, Kahng’s group reported a series self-assembled patterns of brominated anthraquinones on Au(111) surface by Br...Br halogen bonds and $-C-H\cdots Br-C-$ hydrogen bonds.^{38,39} Wu et al. fabricated molecular Sierpiński triangle fractals based on synergistic halogen and hydrogen bonds between two aromatic bromo compounds.³⁵ Deng et al. studied the effects of the position and number of bromine substituents on the 2D self-assembled patterns of phenanthrene derivatives by changing multiple halogen bonds and hydrogen bonds.³¹ It is noteworthy that the halogen elements mentioned above are all bonded to polyaromatic hydrocarbon with C–Br bond. Those bromine elements are constrained to where they are. However, in our work, we use polyaromatic hydrocarbon without any halogen substituents as precursors and apply atomic bromine as a second component to construct the self-assembled molecular networks. The external Br atoms reside themselves into some special positions in molecular networks with maximum number of hydrogen bonds ($-C-H\cdots Br\cdots H-C-$). In addition, no Br...

Br halogen bonds are formed in our systems. The whole 2D chiral halogen-coordinated self-assembly structure can be stabilized by 2D hydrogen-bonding networks. Compared with metal–organic coordination structures,⁴⁰ the halogen–organic coordination network is a new member of 2D layers on surfaces.

In conclusion, we have successfully constructed large-scale, high-quality 2D self-assembled chiral Br-organic networks. The configuration of the network is controlled by the density of Br atoms, substrate and the selected molecule species. We find that the connections between Br atoms and molecules are through $-C-H\cdots Br$ hydrogen bonds. The Br atoms prefer the sites with the maximum number of hydrogen bonds, which serves to stabilize the network. This work provides a prototype for investigating on-surface 2D halogen-coordination networks.

■ ASSOCIATED CONTENT

Supporting Information

The Supporting Information is available free of charge on the ACS Publications website at DOI: 10.1021/acs.jpcllett.6b02680.

Full experimental details; molecules synthetic procedure; height difference of DPA layer and Br atomic layer on Ag(111); and additional STM images about DPA on Cu(111). (PDF)

■ AUTHOR INFORMATION

Corresponding Authors

*X.L.: E-mail: mlin@ucas.ac.cn.

*S.-X.D.: E-mail: sxdu@iphy.ac.cn.

Author Contributions

[§]J.L., D.-L.B., and H.D. contributed equally to this work.

Notes

The authors declare no competing financial interest.

■ ACKNOWLEDGMENTS

We thank Sokrates T. Pantelides and Min Ouyang constructive suggestions. We acknowledge financial support from the National Key Research & Development Projects of China (2016YFA0202300), the National Basic Research Program of China (2013CBA01600), the National Natural Science Foundation of China (Nos. 61390501, 61471337, and 51325204), the CAS Hundred Talents Program, the Transregional Collaborative Research Center TRR 61, and the National Supercomputing Center in Tianjin. A portion of the research was performed in CAS Key Laboratory of Vacuum Physics.

■ REFERENCES

- (1) Thota, B. N.; Uner, L. H.; Haag, R. Supramolecular Architectures of Dendritic Amphiphiles in Water. *Chem. Rev.* **2016**, *116*, 2079–2102.
- (2) Ciesielski, A.; Palma, C.-A.; Bonini, M.; Samori, P. Towards Supramolecular Engineering of Functional Nanomaterials: Pre-Programming Multi-Component 2D Self-Assembly at Solid-Liquid Interfaces. *Adv. Mater.* **2010**, *22*, 3506–3520.
- (3) Gao, H. J.; Gao, L. Scanning Tunneling Microscopy of Functional Nanostructures on Solid Surfaces: Manipulation, Self-Assembly, and Applications. *Prog. Surf. Sci.* **2010**, *85*, 28–91.
- (4) Green, J. E.; Choi, J. W.; Boukai, A.; Bunimovich, Y.; Johnston-Halperin, E.; DeIonno, E.; Luo, Y.; Sheriff, B. A.; Xu, K.; Shin, Y. S.; et al. A 160-Kilobit Molecular Electronic Memory Patterned at 10(11) Bits per Square Centimetre. *Nature* **2007**, *445*, 414–417.

- (5) Rosei, F.; Schunack, M.; Naitoh, Y.; Jiang, P.; Gourdon, A.; Laegsgaard, E.; Stensgaard, I.; Joachim, C.; Besenbacher, F. Properties of Large Organic Molecules on Metal Surfaces. *Prog. Surf. Sci.* **2003**, *71*, 95–146.
- (6) Bartels, L. Tailoring Molecular Layers at Metal Surfaces. *Nat. Chem.* **2010**, *2*, 87–95.
- (7) Barth, J. V.; Costantini, G.; Kern, K. Engineering Atomic and Molecular Nanostructures at Surfaces. *Nature* **2005**, *437*, 671–679.
- (8) Smith, W. F. Organic Electronics-Self-Assembly is Ready to Roll. *Nat. Nanotechnol.* **2007**, *2*, 77–78.
- (9) Zou, Y.; Kilian, L.; Scholl, A.; Schmidt, T.; Fink, R.; Umbach, E. Chemical Bonding of PTCDA on Ag Surfaces and the Formation of Interface States. *Surf. Sci.* **2006**, *600*, 1240–1251.
- (10) Altman, E. I.; Colton, R. J. Nucleation, Growth, and Structure of Fullerene Films on Au(111). *Surf. Sci.* **1992**, *279*, 49–67.
- (11) Baxter, P.; Lehn, J. M.; Decian, A.; Fischer, J. Multicomponent Self-Assembly Spontaneous Formation of a Cylindrical Complex from 5 Ligands and 6 Metal-Ions. *Angew. Chem., Int. Ed. Engl.* **1993**, *32*, 69–72.
- (12) Zheng, Y. R.; Zhao, Z. G.; Wang, M.; Ghosh, K.; Pollock, J. B.; Cook, T. R.; Stang, P. J. A Facile Approach toward Multicomponent Supramolecular Structures: Selective Self-Assembly via Charge Separation. *J. Am. Chem. Soc.* **2010**, *132*, 16873–16882.
- (13) Stepanow, S.; Lingenfelder, M.; Dmitriev, A.; Spillmann, H.; Delvigne, E.; Lin, N.; Deng, X. B.; Cai, C. Z.; Barth, J. V.; Kern, K. Steering Molecular Organization and Host-Guest Interactions Using Two-Dimensional Nanoporous Coordination Systems. *Nat. Mater.* **2004**, *3*, 229–233.
- (14) Seitsonen, A. P.; Lingenfelder, M.; Spillmann, H.; Dmitriev, A.; Stepanow, S.; Lin, N.; Kern, K.; Barth, J. V. Density Functional Theory Analysis of Carboxylate-Bridged Diiron Units in Two-Dimensional Metal–Organic Grids. *J. Am. Chem. Soc.* **2006**, *128*, 5634–5635.
- (15) Cook, T. R.; Zheng, Y. R.; Stang, P. J. Metal–Organic Frameworks and Self-Assembled Supramolecular Coordination Complexes: Comparing and Contrasting the Design, Synthesis, and Functionality of Metal–Organic Materials. *Chem. Rev.* **2013**, *113*, 734–777.
- (16) Langner, A.; Tait, S. L.; Lin, N.; Rajadurai, C.; Ruben, M.; Kern, K. Self-Recognition and Self-Selection in Multicomponent Supramolecular Coordination Networks on Surfaces. *Proc. Natl. Acad. Sci. U. S. A.* **2007**, *104*, 17927–17930.
- (17) Bjork, J.; Matena, M.; Dyer, M. S.; Enache, M.; Lobo-Checa, J.; Gade, L. H.; Jung, T. A.; Stohr, M.; Persson, M. STM Fingerprint of Molecule-Adatom Interactions in a Self-Assembled Metal–Organic Surface Coordination Network on Cu(111). *Phys. Chem. Chem. Phys.* **2010**, *12*, 8815–8821.
- (18) Langner, A.; Tait, S. L.; Lin, N.; Chandrasekar, R.; Ruben, M.; Kern, K. Ordering and Stabilization of Metal–Organic Coordination Chains by Hierarchical Assembly through Hydrogen Bonding at a Surface. *Angew. Chem., Int. Ed.* **2008**, *47*, 8835–8838.
- (19) Tseng, T.-C.; Lin, C.; Shi, X.; Tait, S. L.; Liu, X.; Starke, U.; Lin, N.; Zhang, R.; Minot, C.; Van Hove, M. A.; et al. Two-Dimensional Metal–Organic Coordination Networks of Mn-7,7,8,8-Tetracyanoquinodimethane Assembled on Cu(100): Structural, Electronic, and Magnetic Properties. *Phys. Rev. B: Condens. Matter Mater. Phys.* **2009**, *80*, 155458–155463.
- (20) Schlickum, U.; Klappenberger, F.; Decker, R.; Zoppellaro, G.; Klyatskaya, S.; Ruben, M.; Kern, K.; Brune, H.; Barth, J. V. Surface-Confinement Metal–Organic Nanostructures from Co-Directed Assembly of Linear Terphenyl-Dicarbonitrile Linkers on Ag(111). *J. Phys. Chem. C* **2010**, *114*, 15602–15606.
- (21) Cechal, J.; Kley, C. S.; Kumagai, T.; Schramm, F.; Ruben, M.; Stepanow, S.; Kern, K. Convergent and Divergent Two-Dimensional Coordination Networks Formed through Substrate-Activated or Quenched Alkynyl Ligation. *Chem. Commun.* **2014**, *50*, 9973–9976.
- (22) Xu, W.; Wang, J.-g.; Yu, M.; Lægsgaard, E.; Stensgaard, I.; Linderoth, T. R.; Hammer, B.; Wang, C.; Besenbacher, F. Guanidine and Potassium-Based Two-Dimensional Coordination Network Self-Assembled on Au(111). *J. Am. Chem. Soc.* **2010**, *132*, 15927–15929.

(23) Abdurakhmanova, N.; Floris, A.; Tseng, T. C.; Comisso, A.; Stepanow, S.; De Vita, A.; Kern, K. Stereoselectivity and Electrostatics in Charge-Transfer Mn- and Cs-TCNQ(4) Networks on Ag(100). *Nat. Commun.* **2012**, *3*, 940–946.

(24) Faraggi, M. N.; Jiang, N.; Gonzalez-Lakunza, N.; Langner, A.; Stepanow, S.; Kern, K.; Arnau, A. Bonding and Charge Transfer in Metal–Organic Coordination Networks on Au(111) with Strong Acceptor Molecules. *J. Phys. Chem. C* **2012**, *116*, 24558–24565.

(25) Henningsen, N.; Rurai, R.; Limbach, C.; Drost, R.; Pascual, J. L.; Franke, K. J. Site-Dependent Coordination Bonding in Self-Assembled Metal–Organic Networks. *J. Phys. Chem. Lett.* **2011**, *2*, 55–61.

(26) Sun, Q.; Zhang, C.; Cai, L.; Tan, Q.; Xu, W. Oxygen-Induced Self-Assembly of Quaterphenyl Molecules on Metal Surfaces. *Chem. Commun.* **2014**, *50*, 12112–12115.

(27) Fishlock, T. W.; Pethica, J. B.; Oral, A.; Egdell, R. G.; Jones, F. H. Interaction of Bromine with Ni(110) Studied by Scanning Tunnelling Microscopy. *Surf. Sci.* **1999**, *426*, 212–224.

(28) Basagni, A.; Ferrighi, L.; Cattelan, M.; Nicolas, L.; Handrup, K.; Vaghi, L.; Papagni, A.; Sedona, F.; Di Valentin, C.; Agnoli, S.; et al. On-Surface Photo-Dissociation of C-Br Bonds: towards Room Temperature Ullmann Coupling. *Chem. Commun.* **2015**, *51*, 12593–12596.

(29) O’Connell, M. J.; Eibergen, E. E.; Doorn, S. K. Chiral Selectivity in the Charge-Transfer Bleaching of Single-Walled Carbon-Nanotube Spectra. *Nat. Mater.* **2005**, *4*, 412–418.

(30) Silly, F. Selecting Two-Dimensional Halogen–Halogen Bonded Self-Assembled 1,3,5-Tris(4-iodophenyl)benzene Porous Nanoarchitectures at the Solid–Liquid Interface. *J. Phys. Chem. C* **2013**, *117*, 20244–20249.

(31) Hu, X.; Zha, B.; Wu, Y.; Miao, X.; Deng, W. Effects of the Position and Number of Bromine Substituents on the Concentration-Mediated 2D Self-Assembly of Phenanthrene Derivatives. *Phys. Chem. Chem. Phys.* **2016**, *18*, 7208–7215.

(32) Yasuda, S.; Furuya, A.; Murakoshi, K. Control of a Two-Dimensional Molecular Structure by Cooperative Halogen and Hydrogen Bonds. *RSC Adv.* **2014**, *4*, 58567–58572.

(33) Hipps, K. W.; Scudiero, L.; Barlow, D. E.; Cooke, M. P. A Self-Organized 2-Dimensional Bifunctional Structure Formed by Supramolecular Design. *J. Am. Chem. Soc.* **2002**, *124*, 2126–2127.

(34) Mu, Z.; Shu, L.; Fuchs, H.; Mayor, M.; Chi, L. Two Dimensional Chiral Networks Emerging from the Aryl–F··H Hydrogen-Bond-Driven Self-Assembly of Partially Fluorinated Rigid Molecular Structures. *J. Am. Chem. Soc.* **2008**, *130*, 10840–10841.

(35) Shang, J.; Wang, Y.; Chen, M.; Dai, J.; Zhou, X.; Kuttner, J.; Hilt, G.; Shao, X.; Gottfried, J. M.; Wu, K. Assembling Molecular Sierpinski Triangle Fractals. *Nat. Chem.* **2015**, *7*, 389–393.

(36) Gilday, L. C.; Robinson, S. W.; Barendt, T. A.; Langton, M. J.; Mullaney, B. R.; Beer, P. D. Halogen Bonding in Supramolecular Chemistry. *Chem. Rev.* **2015**, *115*, 7118–7195.

(37) Walch, H.; Gutzler, R.; Sirtl, T.; Eder, G.; Lackinger, M. Material- and Orientation-Dependent Reactivity for Heterogeneously Catalyzed Carbon-Bromine Bond Homolysis. *J. Phys. Chem. C* **2010**, *114*, 12604–12609.

(38) Chung, K. H.; Park, J.; Kim, K. Y.; Yoon, J. K.; Kim, H.; Han, S.; Kahng, S. J. Polymorphic Porous Supramolecular Networks Mediated by Halogen Bonds on Ag(111). *Chem. Commun.* **2011**, *47*, 11492–11494.

(39) Chung, K.-H.; Kim, H.; Jang, W. J.; Yoon, J. K.; Kahng, S.-J.; Lee, J.; Han, S. Molecular Multistate Systems Formed in Two-Dimensional Porous Networks on Ag(111). *J. Phys. Chem. C* **2013**, *117*, 302–306.

(40) Dong, L.; Gao, Z. A.; Lin, N. Self-Assembly of Metal–Organic Coordination Structures on Surfaces. *Prog. Surf. Sci.* **2016**, *91*, 101–135.